



Article

# Network Medicine Approach for Analysis of Alzheimer's Disease Gene Expression Data

David Cohen <sup>†</sup>, Alexander Pilozzi <sup>†</sup> and Xudong Huang <sup>\*†</sup> 

Neurochemistry Laboratory, Department of Psychiatry, Massachusetts General Hospital and Harvard Medical School, Charlestown, MA 02129, USA; dscohen@protonmail.com (D.C.); APILOZZI@mgh.harvard.edu (A.P.)

\* Correspondence: Huang.Xudong@mgh.harvard.edu; Tel./Fax: +1-617-724-9778

<sup>†</sup> These authors contributed equally to this work.

Received: 15 November 2019; Accepted: 30 December 2019; Published: 3 January 2020



**Abstract:** Alzheimer's disease (AD) is the most widespread diagnosed cause of dementia in the elderly. It is a progressive neurodegenerative disease that causes memory loss as well as other detrimental symptoms that are ultimately fatal. Due to the urgent nature of this disease, and the current lack of success in treatment and prevention, it is vital that different methods and approaches are applied to its study in order to better understand its underlying mechanisms. To this end, we have conducted network-based gene co-expression analysis on data from the Alzheimer's Disease Neuroimaging Initiative (ADNI) database. By processing and filtering gene expression data taken from the blood samples of subjects with varying disease states and constructing networks based on that data to evaluate gene relationships, we have been able to learn about gene expression correlated with the disease, and we have identified several areas of potential research interest.

**Keywords:** Alzheimer's disease; network medicine; gene expression; neurodegeneration; neuroinflammation

## 1. Introduction

Alzheimer's disease (AD) is the most widespread diagnosed cause of dementia in the elderly [1]. It is a progressive neurodegenerative disease that causes memory loss as well as other detrimental symptoms and is always fatal. Due to increased lifespans across the globe, this already common disease is expected to become drastically more prevalent in the near future unless intervention occurs. In the United States alone, projections show the prevalence in individuals aged 65 years or older increasing from 4.7 million in 2010 to 13.8 million in 2050 [2]. At the present time, a wide variety of research is being conducted in order to counteract the growing AD epidemic; despite this, there is currently no known effective method of treatment or prevention. Researchers are exploring this disease from many different perspectives in order to better understand its underlying mechanisms responsible for it [3]. In this paper, the application of network medicine (NM) on AD will be explored. NM is a constantly developing field of research that strives to connect the various genetic, molecular and environmental drivers of diseases such as AD to as many involved components as possible. Ideally, having a more complete picture of disease-related pathways will grant more avenues for potential treatment than reducing the problem to single components or genes [4]. A significant focus of network medicine involves inspecting the complex interactions between genes underlying diseases, such as AD [5–7]. Diseases occur at varying biological complexities and therefore it is crucial to understand the networks of genes underlying a disease. The more holistic approach of NM advances drug targeting by eliminating the reliance on single components or genes, and instead allows for targeting networks of interacting components or genes. It also allows for the analysis of potential off target effects, which is very useful for drug development. NM can provide very insightful results on datasets such as gene

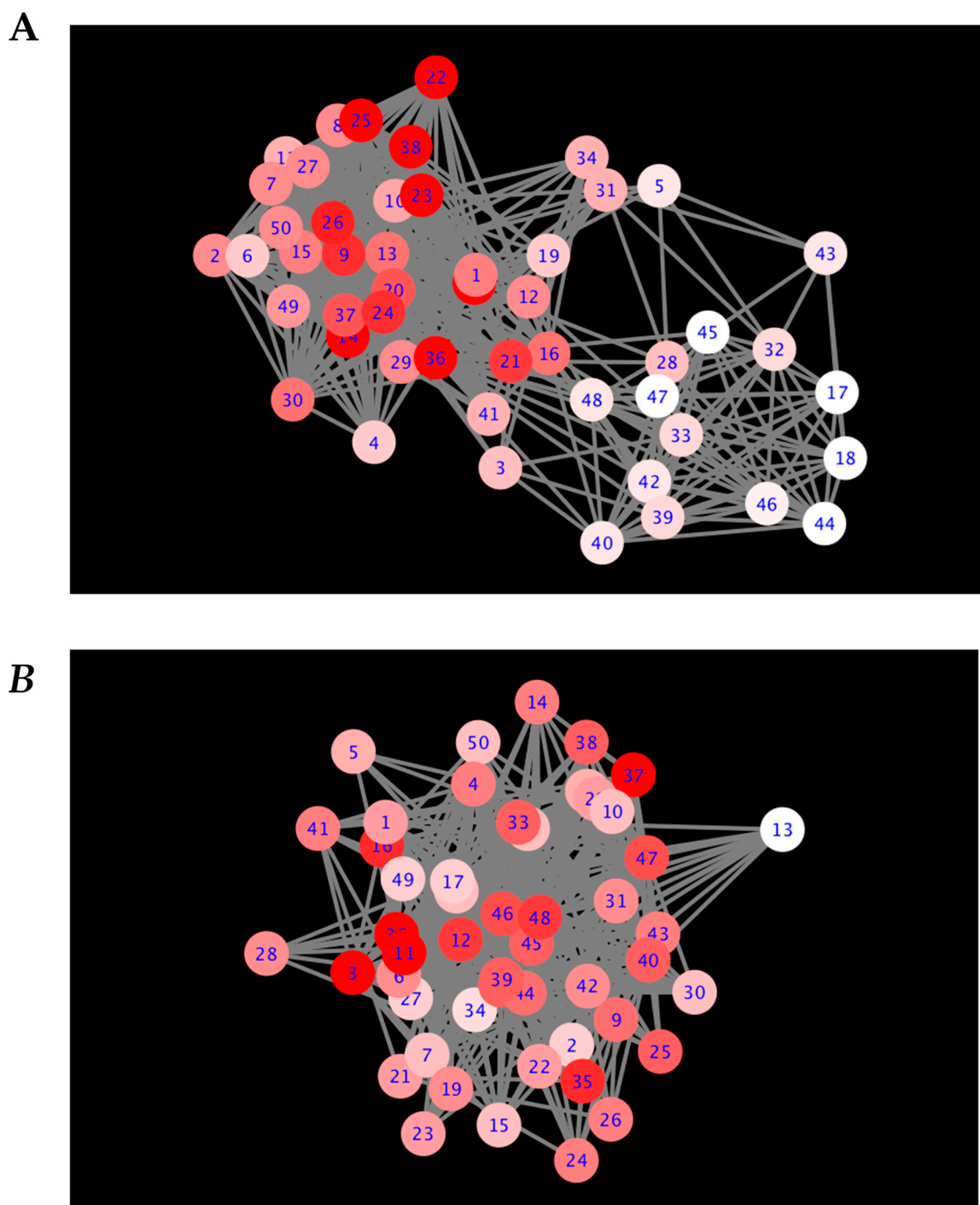
expression data [8,9]. While studies involving gene expression data from AD patients are not rare, there are comparatively few that conduct network-based analysis on that data. Much of the work involving Alzheimer's related network analysis apply the techniques to protein interactomes [10,11] or the interactomes of existing drugs/drug-targets [12]. Of some involved in co-expression analysis, Mostafavi et al. constructed networks based on expression data obtained from the dorsolateral prefrontal cortex of nonaffected individuals and those afflicted with mild cognitive impairment (MCI) or AD; genes were clustered into, and analyzed as, modules [13]. Here, we examine co-expression based on blood samples, looking at transcript-level interactions found in a heavily filtered subset of the expression data.

## 2. Results

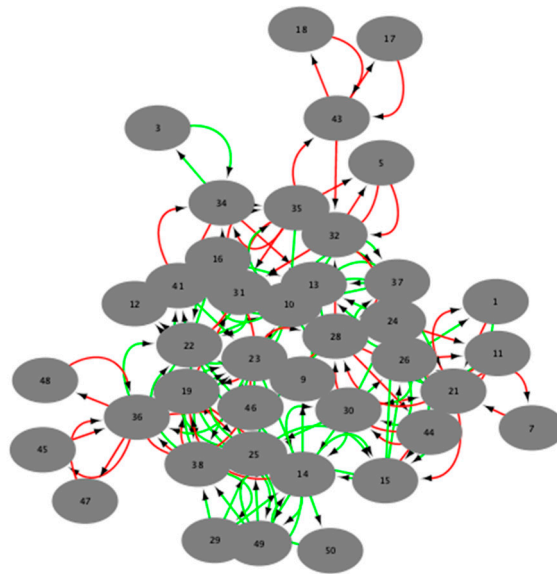
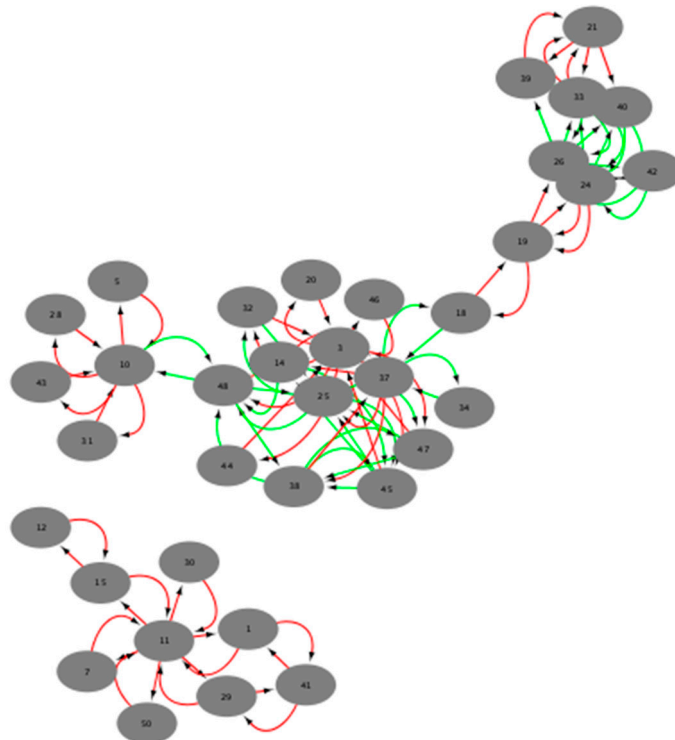
Figure 1A is the visual representation of the DyNet network associated with positive gene expression correlations. Figure 1B is the visual representation of the DyNet network associated with negative gene expression correlations. Figure 2A is the visual representation of the Diffany network associated with positive gene expression correlations. Figure 2B is the visual representation of the Diffany network associated with negative gene expression correlations. Figures 3 and 4 are the simple correlation networks for the different disease states ordered by correlation type. All networks are included as Supplementary Materials. All numbers correspond to genes in Table 1 by key. The 49,293 transcripts from the original expression dataset were filtered in two stages, using ANOVA (groups were NC, MCI, AD,  $p < 0.1$ ) and additional thresholds for expression level. The final number of transcripts passing filtration was 50. These 50 genes are described in Table 1. Transcript names that are repeated in the dataset represent transcripts that are associated with multiple. The probe set ID for each transcript is listed below its name. Differences in expression levels relative to NC are listed, with  $p$  values for the differences that are greater than 0.1 shown below the overall direction of relative expression. A "-" indicates the  $p$  value exceeded 0.75, regardless of direction (Welch  $t$ -test, FDR adjusted  $p$  value).

Looking at Table 1, we can see that in many of the genes that are significantly upregulated and downregulated in AD individuals are regulated in the same direction in MCI individuals, though there are some notable exceptions such as haptoglobin, along with genes whose expression changes are not necessarily significant between the NC and MCI states.

From the correlation matrices generated from the expression data of the genes in Table 1, DyNet networks were generated. These networks indicate nodes whose connections change between states (i.e., connections in one network that are not present in the other network or network). The deep red nodes, such as the haptoglobin transcript node #38, experience a greater degree of connectivity disruption (i.e., connections added or removed) between the different disease states. The light red/white nodes experience more consistent connection (i.e., few connections added or removed) between the different disease states. Edges are present in the DyNet networks where any network (NC, MCI, or AD) has an edge.



**Figure 1.** DyNet networks. The deeper the red of the node, the more rewiring has occurred. DyNet calculates the variance between each node's connectivity between networks and computes a score based on the number of altered (i.e., added, removed) connections. Based on Pearson coefficient threshold  $T = 0.1$  networks. (A) Positive Pearson correlation DyNet network. (B) Negative Pearson correlation DyNet network.

**A****B**

**Figure 2.** Diffany networks. Green arrows represent increase in association and red indicate decrease in association between genes (Alzheimer’s disease (AD)/MCI vs. NC). Association is determined by the addition or removal of edges between networks in comparison to a reference condition. Based on Pearson coefficient threshold  $T = 0.1$  networks. **(A)** Diffany network generated from positive correlation networks. **(B)** Diffany network generated from negative correlation networks.

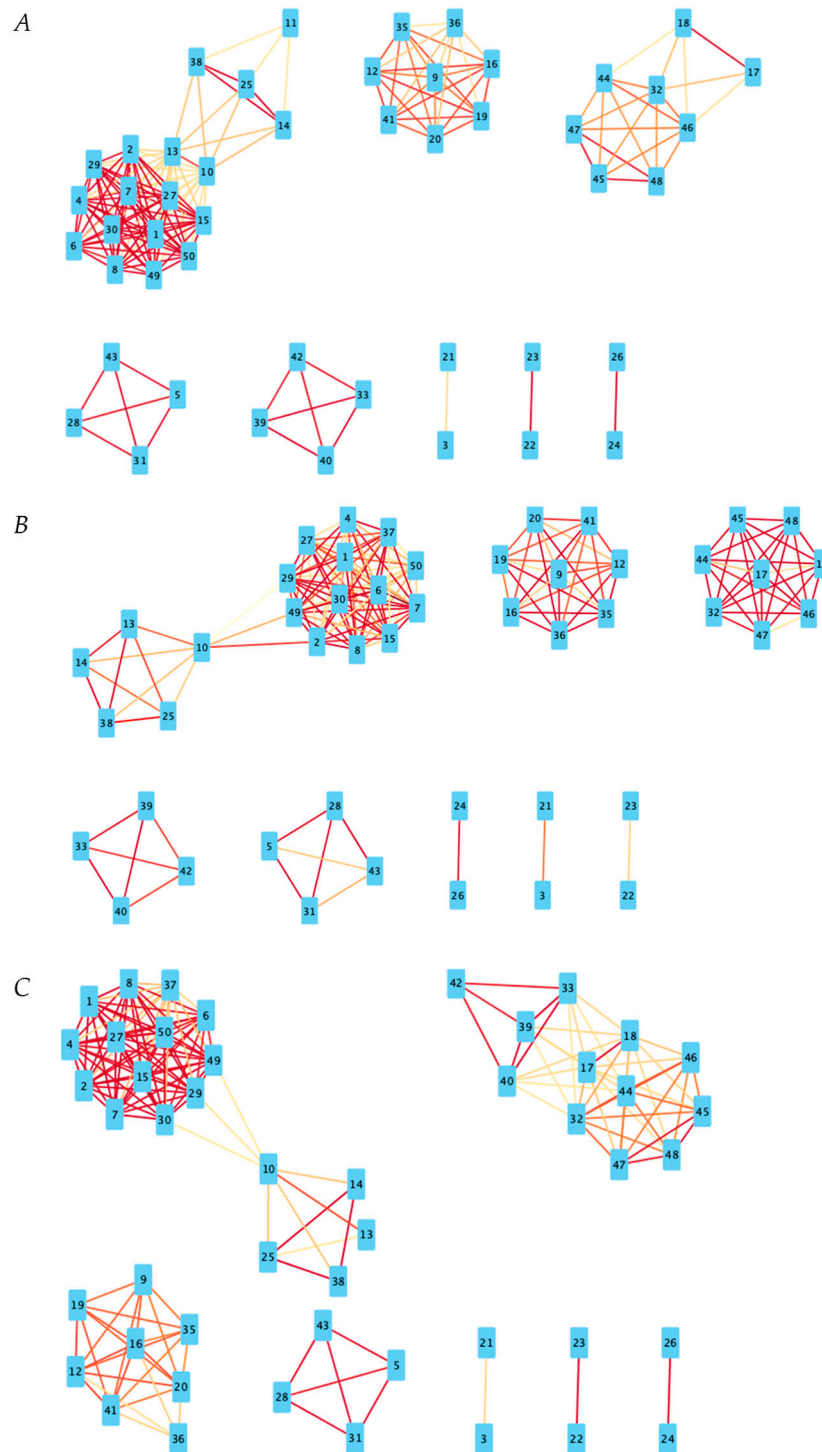


**Figure 3.** Positive correlation networks for all disease states. Red lines indicate a higher Pearson Correlation coefficient. Based on Pearson coefficient threshold  $T = 0.3$  networks. **(A)** Positive correlation network for NC state. **(B)** Positive correlation network for MCI state. **(C)** Positive correlation network for AD state.

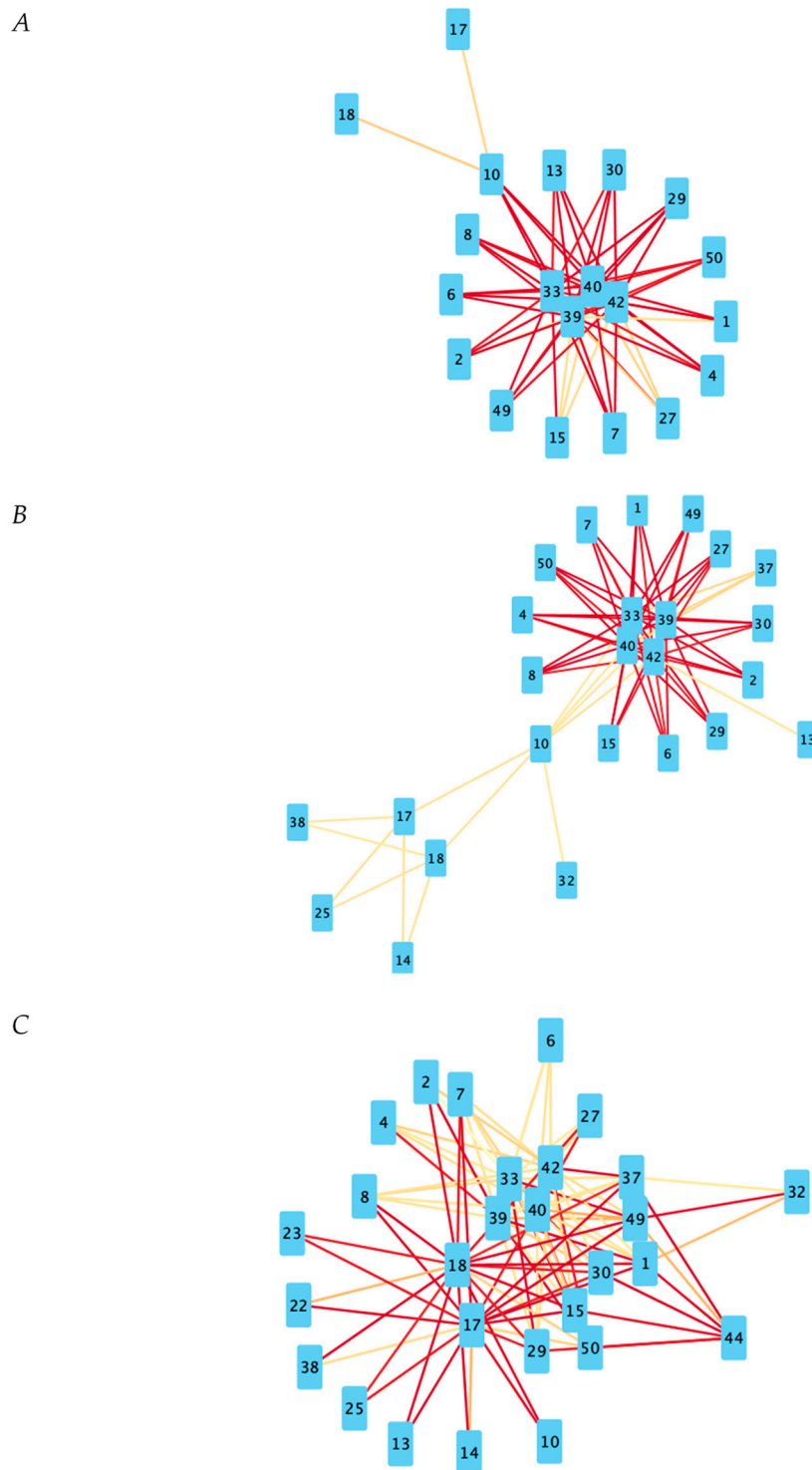


**Figure 4.** Negative correlation networks for all disease states. Red lines indicate a higher Pearson correlation coefficient. Based on Pearson coefficient threshold  $T = 0.3$  networks. (A) Negative correlation network for NC state. (B) Negative correlation network for MCI state. (C) Negative correlation network for AD state.

**Table 1.** Genes selected using genefilter | Expression Rel. to NC <sup>1</sup>.

Key	Gene	Expression in MCI <sup>2</sup>	Expression in AD
1	[RPS4Y1] Ribosomal protein S4 Y-linked 1 Probe set: 11716411_x_at	Up	Up
2	[EIF1AY] eukaryotic translation initiation factor 1A Y-linked Probe set: 11720807_x_at	Up	Up
3	[GATA2] GATA binding protein 2 Probe set: 11722761_a_at	Down	Down $p = 0.203$
4	[DDX3Y] DEAD (Asp-Glu-Ala-Asp) box helicase 3 Y-linked Probe set: 11724075_a_at	Up	Up
5	[HLA-DQA1] Major histocompatibility complex class II DQ alpha 1 Probe set: 11724799_x_at	Up	Up $p = 0.694$
6	[USP9Y] ubiquitin specific peptidase 9 Y-linked Probe set: 11725294_at	Up	Up $p = 0.194$
7	[KDM5D] lysine (K)-specific demethylase 5D Probe set: 11726813_a_at	Up	Up
8	[KDM5D] lysine (K)-specific demethylase 5D Probe set: 11726814_x_at	Up	Up
9	[TBC1D22B] TBC1 domain family member 22B Probe set: 11728078_a_at	Up $p = 0.670$	Down
10	[BPI] Bactericidal/permeability-increasing protein Probe set: 11729344_at	Up $p = 0.225$	Up
11	[ANKRD22] Ankyrin repeat domain 22 Probe set: 11732425_at	Up $p = 0.334$	Up
12	[TMOD1] Tropomodulin 1 Probe set: 11732501_a_at	Down $p = 0.587$	Down
13	[DEFA4] Defensin alpha 4 corticostatin Probe set: 11732546_at	Up $p = 0.293$	Up
14	[HP] Haptoglobin Probe set: 11733829_x_at	- $p = 0.991$	Up
15	[DDX3Y] DEAD (Asp-Glu-Ala-Asp) box helicase 3 Y-linked Probe set: 11734664_x_at	Up	Up
16	[OSBP2] Oxysterol binding protein 2 Probe set: 11736205_a_at	Down $p = 0.473$	Down
17	[FCRL1] Fc receptor-like 1 Probe set: 11736882_a_at	Down $p = 0.641$	Down
18	[FCRL1] Fc receptor-like 1 Probe set: 11736883_x_at	Down $p = 0.694$	Down
19	[FAM46C] Family with sequence similarity 46 member C Probe set: 11739338_at	Down $p = 0.531$	Down
20	[OR2W3] (Locus via Non-standard RNA) olfactory receptor family 2 subfamily W member 3 Probe set: 11741636_at	- $p = 0.843$	Down
21	[CACNG6] Calcium channel voltage-dependent gamma subunit 6 Probe set: 11742124_a_atex	Down	Down $p = 0.616$
22	[FOLR3] folate receptor 3 (gamma) Probe set: 11744140_a_at	Up $p = 0.645$	Up $p = 0.163$
23	[FOLR3] folate receptor 3 (gamma) Probe set: 11744141_x_at	Up $p = 0.582$	Up $p = 0.137$

Table 1. Cont.

Key	Gene	Expression in MCI <sup>2</sup>	Expression in AD
24	[CBS] Cystathionine-beta-synthase Probe set: 11744286_s_at	- $p = 0.995$	Up
25	[HP] Haptoglobin Probe set: 11744649_x_at	- $p = 0.76$	Up $p = 0.141$
26	[CBS] Cystathionine-beta-synthase Probe set: 11744835_s_at	- $p = 0.995$	Up
27	[KDM5D] lysine (K)-specific demethylase 5D Probe set: 11745012_a_at	Up	Up
28	[HLA-DQB1] Major histocompatibility complex class II DQ beta 1 Probe set: 11746804_x_at	Up	Up $p = 0.46$
29	[DDX3Y] DEAD (Asp-Glu-Ala-Asp) box helicase 3 Y-linked Probe set: 11748424_x_at	Up	Up
30	[DDX3Y] DEAD (Asp-Glu-Ala-Asp) box helicase 3 Y-linked Probe set: 11749841_x_at	Up	Up
31	[HLA-DQA1] Major histocompatibility complex class II DQ alpha 1 Probe set: 11750528_x_at	Up	- $p = 0.89$
32	[ENSG00000211625    ENSG00000239951] (Matches 2 Loci; Matches Ensembl Gene) Putative uncharacterized protein ENSP00000374805 [Source:UniProtKB/TREMBL;Acc:A6NLY3]    Ig kappa chain V-III region HAH Precursor [Source:UniProtKB/Swiss-Prot;Acc:P18135] Probe set: 11753832_x_at	Down $p = 0.123$	Down
33	[XIST] X inactive specific transcript (non-protein coding) Probe set: 11754194_s_at	Down	Down
34	[EGR1] Early growth response 1 Probe set: 11754334_s_at	Down	Down
35	[NUDT4    NUDT4P2    NUDT4P1] (Matches 3 Loci) Nudix (Nucleoside diphosphate linked moiety X)-type motif 4    nudix (nucleoside diphosphate linked moiety X)-type motif 4 pseudogene 2    Nudix (nucleoside diphosphate linked moiety X)-type motif 4 pseudogene 1 Probe set: 11754453_s_at	- $p = 0.846$	Down
36	[SHISA4] shisa family member 4 Probe set: 11756240_a_at	Down $p = 0.641$	Down
37	[PTGDS] prostaglandin D2 synthase 21kDa (brain) Probe set: 11756587_a_at	- $p = 0.853$	Up
38	[HP] Haptoglobin Probe set: 11757277_x_at	- $p = 0.932$	Up
39	[XIST] X inactive specific transcript (non-protein coding) Probe set: 11757733_s_at	Down	Down
40	[XIST] X inactive specific transcript (non-protein coding) Probe set: 11757857_s_at	Down	Down
41	[TRIM10] tripartite motif containing 10 Probe set: 11758611_s_at	Up $p = 0.647$	Down

Table 1. Cont.

Key	Gene	Expression in MCI <sup>2</sup>	Expression in AD
42	(Matches Non-standard RNA) JARID1C protein (JARID1C) mRNA complete cds alternatively spliced Probe set: 11761133_at	Down	Down
43	[HLA-DQB1] (POOR HIT 44%) Major histocompatibility complex class II DQ beta 1 Probe set: 11762641_x_at	Up	Up $p = 0.56$
44	(DEPRECATED TARGET; Matches RefSeq) (Deprecated) PREDICTED: Homo sapiens similar to <i>hCG2042707</i> (LOC650405)    (Deprecated) PREDICTED: Homo sapiens similar to pre-B lymphocyte gene 1 (LOC652493)    (Deprecated) PREDICTED: Homo sapiens similar to <i>hCG26659</i> (LOC100291464) Probe set: 11763222_x_at	Down $p = 0.316$	Down
45	[ENSG00000211663] (Matches Ensembl Gene) V2-13 protein Fragment [Source:UniProtKB/TrEMBL; Acc:Q5NV73] Probe set: 11763229_x_at	Down $p = 0.331$	Down
46	[ENSG00000242534    ENSG00000244116] (Matches 2 Loci; Matches Ensembl Gene) immunoglobulin kappa variable 2D-28 [ENST00000453166 ENST00000558026]    immunoglobulin kappa variable 2-28 [ENST00000482769]	Up $p = 0.614$	Down $p = 0.122$
47	[ENSG00000211663] (Matches Ensembl Gene) V2-13 protein Fragment [Source:UniProtKB/TrEMBL;Acc:Q5NV73] Probe set: 11763255_x_at	Down $p = 0.279$	Down
48	[ENSG00000211663] (Matches Ensembl Gene) V2-13 protein Fragment [Source:UniProtKB/TrEMBL;Acc:Q5NV73] Probe set: 11763551_x_at	Down $p = 0.332$	Down
49	(Matches Non-standard RNA) mRNA; cDNA DKFZp686L12190 (from clone DKFZp686L12190): Probe set: 11763837_s_at	Up	Up
50	[TXLNG2P] (Matches Ensembl Gene) Uncharacterized protein CYorf15B (Lipopolysaccharide-specific response 5-like protein) [Source:UniProtKB/Swiss-Prot;Acc:Q9BZA4] Probe set: 11764064_s_at	Up	Up

<sup>1</sup> NC—normal condition. <sup>2</sup> MCI—mild cognitive impairment.

Table 2 contains the top rewiring scores for the DyNet network associated with positive gene expression correlations. Table 3 contains the top rewiring scores for the DyNet network associated with negative gene expression correlations. Both tables were cut off at the score of 5. Some genes with scores lower than five were considered for further analysis; those with scores nearing five were taken into consideration, one such gene being OSBP2.

**Table 2.** DyNet top positive rewiring genes.

Gene	DyNet Rewiring Score
[HP] Haptoglobin Probe set: 11757277_x_at	8.33
[FOLR3] folate receptor 3 (gamma) Probe set: 11744141_x_at	8.00
[FOLR3] folate receptor 3 (gamma) Probe set: 11744140_a_at	8.00
[NUDT4    NUDT4P2    NUDT4P1] (Matches 3 Loci) Nudix (Nucleoside diphosphate linked moiety X)-type motif 4    nudix (nucleoside diphosphate linked moiety X)-type motif 4 pseudogene 2    Nudix (nucleoside diphosphate linked moiety X)-type motif 4 pseudogene 1HP Probe set: 11754453_s_at	7.00
[HP] Haptoglobin Probe set: 11744649_x_at	7.00
[HP] Haptoglobin Probe set: 11733829_x_at	7.00
[SHISA4] shisa family member 4 Probe set: 11756240_a_at	6.67
[CBS] Cystathionine-beta-synthase Probe set: 11744835_s_at	6.00
[TBC1D22B] TBC1 domain family member 22B Probe set: 11728078_a_at	5.67
[CBS] Cystathionine-beta-synthase Probe set: 11744286_s_at	5.67

**Table 3.** DyNet top negative rewiring genes.

Gene	DyNet Rewiring Score
[GATA2] GATA binding protein 2 Probe set: 11722761_a_at	8.00
[PTGDS] prostaglandin D2 synthase 21kDa (brain) Probe set: 11756587_a_at	6.33
[ANKRD22] Ankyrin repeat domain 22 Probe set: 11732425_at	6.33
[SHISA4] shisa family member 4 Probe set: 11756240_a_at	5.67

To determine the differences in co-expression relative to NC individuals that are common to both MCI and AD participants, Diffany networks were constructed. A red edge indicates that an edge present in the NC network is absent in both the MCI and AD networks. A green edge indicates that an edge absent in the NC network is present in both the MCI and AD networks. From the positive co-expression Diffany network (Figure 2A), we can find that certain transcripts such as folate receptor 3 (#23) gain positive co-expression-relationships to a host of different transcripts in MCI and AD participants whereas one MHC transcript (#31) loses positive co-expression relationships. Many other transcripts exhibit combinations of gained and lost relationships.

The negative co-expression Diffany network (Figure 2B) follows the same principles as the positive co-expression network; green edges indicate a negative co-expression relationship present in only the MCI and AD networks, while red edges indicate a negative co-expression relationship absent in only

the MCI and AD networks. From this network, we find that transcripts such as *ANKRD22* (#11) are no longer negative co-expressed with several other transcripts such as the three *DDX3Y* (#15, #29, #30) and one *KDM5D* (#7) transcript in the MCI and AD states. While there are no transcripts that purely gain negative co-expression relationships, transcripts such as the two V2-13 protein fragments commonly gain negative co-expression relationships with the three haptoglobin transcripts (#14, # 25, #38) and lose negative co-expression relationships with *GATA2* (#3).

For the purpose of examining the general co-expression relationships between genes, three additional co-expression networks for created with a correlation threshold of 0.3 to eliminate the weakest correlations; transcripts (nodes) with correlation coefficients above 0.3 in the positive correlation networks and below  $-0.3$  in the negative correlation networks have an edge between them. Red edges indicate higher absolute-value Pearson coefficients of correlation than more yellow edges (i.e., 0.9 and  $-0.9$  will appear more deeply red than 0.4 and  $-0.4$ , respectively).

### 3. Discussion

#### 3.1. Network Medicine Applied to Gene Expression Data

Through the mapping out of these genes in networks, we can better understand their relations to MCI and AD. The effectiveness of the network comparison tools utilized is supported by our results. Many of the genes that are duplicates/of the same family have similar rewiring scores; all of the instances of haptoglobin (*HP*), for example, have rewiring scores between 7 and 8.33 relative to the positive-correlation networks. These same groupings of genes are not connected in the Diffany networks, indicating that the relationships between them, which should be very strong, are not disrupted between disease states. Furthermore, while they themselves are not connected, gene families/groups have many other common gene connections, indicating they experience many of the same correlational changes between disease states.

It is demonstrated that an effective method was followed for gene selection due to the nature of some of the genes observed; many of the genes found to be significant have well-studied mechanisms for contributing to AD, and many others have significant regulatory function or are commonly expressed in the brain.

#### 3.2. Highly Disrupted Genes

Of the overexpressed genes, haptoglobin, which had the highest rewiring score between the positive correlation networks, has been shown to be affected by AD in previous research [14]. Indeed, serum levels of HP are observed in significantly higher quantities in individuals with AD as well as MCI [15]. It is known to be partially responsible for suppressing certain types of inflammatory responses [16]. Inflammation, both systemic and localized to the central nervous system, is widely accepted to be a contributor to Alzheimer's disease [17]. The fact that it is only expressed in AD patients may be due to it is released in response to AD-specific inflammation.

Folate receptor 3 (gamma) is another gene of interest that exhibited a high degree of correlational disruption. It encodes a member of the folate receptor family of proteins, which have a high affinity for folic acid and folate intake has been correlated with reduced risk of AD [18]. Folate deficiency contributes to hyperhomocysteinemia, which is a risk factor for Alzheimer's as well as other neurological disorders [19].

*OSBP2* is a gene whose product binds to Oxysterol, which is known for its contribution to cholesterol disequilibrium. High cholesterol is a known risk factor for Alzheimer's disease, but cholesterol itself cannot penetrate the blood brain barrier, making the mechanism by which hypercholesterolemia contributes to the disease somewhat obscure. On the other hand, oxysterols, which are oxidized cholesterol metabolites, are able to enter the brain [20].

Cystathionine beta synthase (CBS) has been shown to be associated with AD due to its role in homocysteine metabolism. It, in conjunction with two other enzymes, is responsible for the metabolism

of homocysteine, with accumulation of homocysteine, hyperhomocysteinemia, being a known risk factor for AD [21]. CBS is notably overexpressed in individuals with Alzheimer's disease, indicating the possibility that some other portion of the cysteine metabolic pathway is disrupted, and an increase in CBS is a response. Additionally, the metabolic activity of CBS increases levels of H<sub>2</sub>S, which is known to be neuroprotective, in the brain [22].

*TBC1D22B* is a gene with a notable TBC domain; within the networks it experienced a fairly high degree of connection disruption based on DyNet. TBC domain proteins are primarily GTPase activating proteins for the small GTPase Rab, and defective TBC proteins are implicated in a variety of human diseases. As GTPase activity is a regulator of other cellular functions, those genes regulated by *TBC1D22B* are of interest as potential contributors to AD and MCI [23].

For negatively expressed genes, GATA binding protein 2 is known to be an essential transcription factor for neuroglobin; *GATA-2* knockdown causes significant drops in neuroglobin expression. Neuroglobin has been observed to have a protective effect on neural cells and has been implicated in reducing the severity of AD [24]. It experiences the most rewiring relative to the negative correlation networks. Tropomodulin, a regulator of actin, has been found to be important to the proper development of neural dendrites [25]. As a final example shisa member family 4 is more esoteric than some of the other genes but is shown to be highly expressed in the brain [26].

### 3.3. Notable Connections and Clusters

#### 3.3.1. Y-Linked Regulators

While those genes highlighted by the DyNet and Diffany networks are certainly significant and show some unique patterns of correlation disruption between NC, MCI, and AD conditions, the primary utility of network mapping is to highlight strong relationships between genes. Notably, some genes were excluded entirely in both the positive and negative correlation Diffany networks. These genes have many connections within the base networks but are notably genes associated with basic cellular function. These include: *EIF1AY*, *DDX3Y*, *USP9Y*, and *KDM5D*. *EIF1AY* is a gene located on the Y chromosome, which encodes a translation initiation factor thought to stabilize the binding of initiation Met-tRNA to the ribosome [27]. *DDX3Y* is a gene located on the Y chromosome that encodes a member of the DEAD-box RNA helicase family that is active in male germ cells [28]. The third member of this group of Y-linked genes is *USP9Y*, which is a protease which cleaves ubiquitin from ubiquitinated proteins and ubiquitin-fused precursors [29]. The last of the Y-linked genes in this set is *KDM5D*, which is a male lysine-specific histone demethylase that regulates transcription factors that modulate the cell cycle [30]. As one might expect of these four genes, they are all directly connected on the positive-correlation networks of every disease condition, and all three are over-expressed in both MCI and AD individuals.

Looking at all three networks of positively correlated genes, there is a notable network of over 13 genes which are all related to each other. This group is mostly comprised of duplicates/variants of the Y-linked genes mentioned above, along with an additional Y-linked gene, *RPS4Y1*, which codes for a ribosomal protein [31]. All of these genes are in some fashion, be it direct-involvement or regulation, related to the gene expression process, are Y-linked and are themselves overexpressed in individuals with Alzheimer's disease. The other items in this cluster are largely unidentified transcripts; perhaps their connection to the other Y-linked genes may aid in their identification.

Interestingly, in NC individuals the levels of Prostaglandin D2 synthase (*PTGDS*) expression are not significantly correlated to any gene in this study. However, in both the MCI and AD conditions, it is correlated to the entire cluster of Y-linked genes, albeit at only a moderate level. Prostaglandin is notable for being active in nervous system development and regeneration processes [32].

### 3.3.2. Immune-System Involved

While the previously mentioned cluster is present in all three disease states, it is more well-defined in MCI and AD patients. In NC individuals, the cluster mixes with another that is normally mediated by the *BPI* (bactericidal/permeability-increasing protein) gene, which is a hub between two clusters in the MCI and AD condition networks. Notably, this hub contains the aforementioned *BPI* gene, as well as the haptoglobin genes (*HP*) and the *DEFA4* gene. *BPI* and *DEFA4* both code for components of the immune system; the latter is a defensin, which are known for disrupting microbial membranes, while the former is a protein involved in enhancing immune-cell bacterial recognition [33,34]. There may in fact be a connection between these immune genes and the haptoglobin gene, as findings suggest that haptoglobin has a role in the regulation of the immune system; haptoglobin deficient mice have a reduction in the presence of T and B cells, and they exhibit overall inhibited adaptive immune responses [35]. The immune system is known to have an impact on the pathogenesis of Alzheimer's disease, making the aforementioned immune components, alongside other related pathways and regulators, a worthy target for future investigation [36]. It is unclear whether defensin's connection to the greater translation cluster is a coincidence, or if their pathways are linked in some way; it is also unclear why this linkage seems to be more prevalent in those afflicted with any degree of cognitive impairment than cognitively normal individuals.

A somewhat related cluster involved in all three disease states contains the four transcripts associated with some portion of the Major Histocompatibility Complex (MHC). The MHC is responsible for presenting antigens along the cell surface for T-cell recognition [37]. While the relationship between the four is preserved throughout the three disease states, it breaks down somewhat in AD individuals, with the gene only identified to be somewhat related to the MHC (44% BLAST hit) becoming less correlated with the others. Also, it should be mentioned that overexpression of these MHC transcripts is far less significant in AD patients than in MCI patients, with substantial differences between the alpha and beta transcripts. Regardless, it further reinforces the idea that the immune system has an important role to play in the progression of cognitive decline, as the various immune-system related genes in the set studied are all overexpressed in AD patients.

### 3.3.3. Under Expressed Regulatory Elements

Looking to the networks of negative correlations, there appear to be fewer hubs of interest than in the positive correlation networks. Central hubs of the networks for all three disease states include three instances of X-inactive specific transcript (*XIST*), which is downregulated in both MCI and AD individuals. *XIST* is a regulatory long non-coding RNA (lncRNA); *XIST* notably is involved in X-inactivation in females, possibly explaining why there are fairly consistent negative correlations between it and the Y-linked genes [38]. lncRNAs in general have been implicated in the pathogenesis of Alzheimer's disease that are both up and down regulated in the disease [39]. Another hub that is present in all three is a *JARID1C* splice variant. *JARID1C* is integral to heterochromatin formation and replication. As heterochromatin cannot be transcribed, inhibiting its formation through the downregulation of *JARID1C* may be a potential mechanism for the overexpression of the host of genes connected to it [40]. Both *XIST* and *JARID1C* are known regulators of neural development and have been implicated in other neural/intellectual disorders [41]. Notably, the three *XIST* genes and the *JARID1C* gene are connected to most of the same genes in all three negative correlation networks; additionally, these correlations seem to weaken in AD subjects specifically, indicating potential interference by a competing regulatory pathway. Additionally, all four are themselves a separate non-connected subgraph on all three positive correlation networks, indicating that the expression of *XIST* and *JARID1C* are linked in some way, and whatever mutually regulates their expression may be a target of interest for future research.

### 3.3.4. Folate Receptors

Aside from this central cluster of four genes in the negative-correlation networks, there is a pattern of interest involving the two folate receptor genes. While these genes are only present on the network of NC individuals based on relatively weak correlations to *DEFA4*, it becomes far more connected from MCI to AD individuals; they are connected to the three genes for *HP* as well as Defensin in MCI individuals with moderate correlations, and they are connected to over 17 different genes in AD patients with relatively strong correlations. Why the folate receptor is so central to the negative-correlation network in AD patients is unclear, though folate does have cited benefits against AD [18].

### 3.3.5. Unidentified Transcripts

Another cluster of interest involves the majority of the unidentified/partially identified genes/gene products. In all three networks, these genes fully connected to each other and to both instances of the folate receptor gene. This could prove useful in further identification of the genes, and they may prove to be relevant to Alzheimer's research given folate's protective benefits against the disease [18].

## 4. Materials and Methods

### 4.1. Alzheimer's Disease Neuroimaging Initiative

Data used in this paper originates from the Alzheimer's Disease Neuroimaging Initiative (ADNI) database ([adni.loni.usc.edu](http://adni.loni.usc.edu)). The ADNI was launched in 2003 as a public-private partnership, led by Principal Investigator Michael W. Weiner, MD. An overarching goal has been for the ADNI to provide a collection of multi-categorical data that researchers can utilize in order to better understand mild cognitive impairment (MCI) and AD. The ADNI has recruited over 800 adults, aged 55 to 90 from sites spanning both the US and Canada. In the initial stage of the study, approximately 200 cognitively normal individuals were followed for three years, 400 subjects with MCI were followed for three years, and 200 patients with early AD were followed for two years [42]. The project has gone on to involve further studies, adding in additional subjects and continuing the observation of previous participants [43]. ADNI data spans different categories including clinical data, MR image data, PET image data, genetics data, and biospecimen data. For the purpose of creating the network, gene expression data extracted from the participants' blood samples will be the primary form of data used in this paper. Gene expression profiles were taken from 811 ADNI participants using the Affymetrix Human Genome U219 Array. Sixty-four samples were removed from the dataset as they did not pass quality control checks [44].

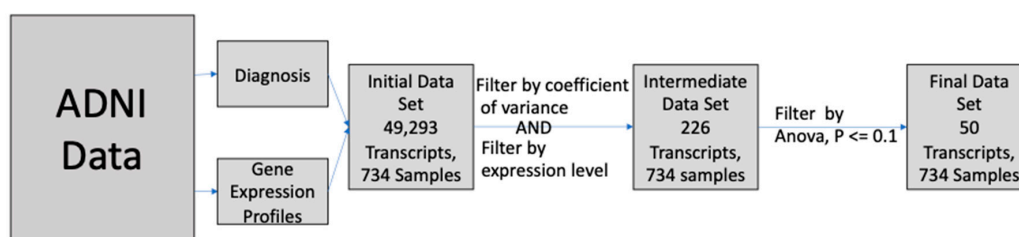
### 4.2. Network Medicine Applied to AD Gene Expression Data

For the network medicine analysis, microarray gene expression data was utilized in tandem with a diagnosis dataset. In order to properly utilize these data, diagnosis status (NC, MCI, or AD) was merged with the expression dataset. The diagnosis given on or nearest to the date of gene expression collection was assigned to each participant. The data was also cleaned prior to use. The gene expression dataset contains 49,386 expression data points per participant, with each point consisting of a gene expression level value for a given gene. Seven hundred and forty-four participants with corresponding diagnosis and expression data were utilized. The goal of the implementation was to separate gene expressions by diagnosis (NC, MCI, and AD), build a network for each condition, and compare networks. With 49,386 samples per participant, the full set of correlation values became extremely large, so the data needed to be filtered. This was done using Bioconductor's *genefilter* R utility (<http://www.bioconductor.org/packages/release/bioc/html/genefilter.html>). Genes were kept if they had both a coefficient of variation between 0.7 and 10, and if 20% or more samples exhibited an expression level greater than 100 for that gene [45]. Because data was normalized using the RMA (Robust Multi-chip Average) normalization method, the normalization and the log-scaling was reversed for the calculations. Bioconductor's *genefilter* was also used to run an ANOVA between

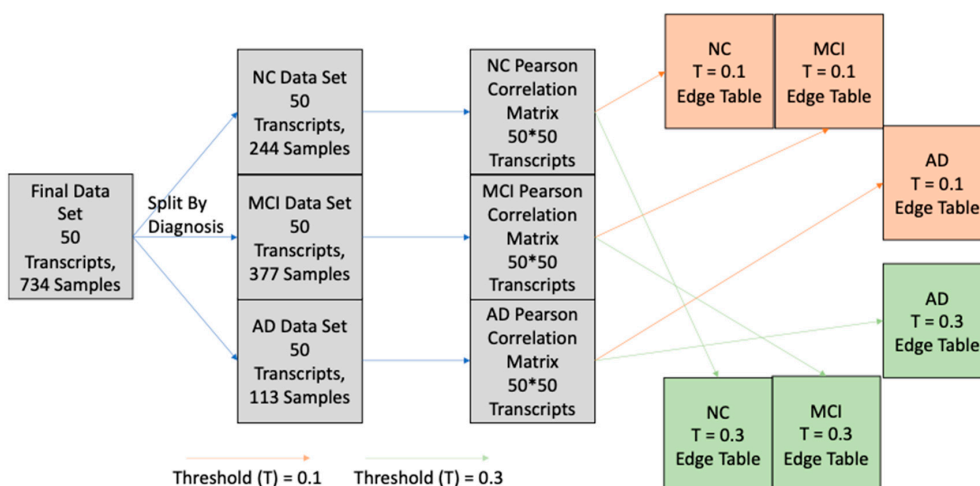
groups and apply a filter, keeping genes with the most significant differences between conditions. Fifty genes passed both filtering stages. A list of these genes is available in Table 1, along with their overall expression change in AD and MCI participants relative to NC participants.  $p$  values for these expression changes are listed if they exceeded 0.1. Three Pearson Correlation matrices were generated for both positive and negative correlations between genes of the different conditions (NC, MCI, and AD), resulting in six total matrices. Thresholds were applied to the correlation matrices in order to filter out the very weak relationships. For the purpose of analyzing relationship-disruptions between disease states, a threshold of 0.1 was applied to filter out very weak or non-correlations. For the purpose of directly examining the relationships between genes, a threshold of 0.3 was applied to filter out the weak correlations.

Networks were then generated in Cytoscape [46]. In order to better understand these networks, two complementary visual analysis tools were used. DyNet is a tool that compares two or more networks with the same node-set and identifies the nodes whose connections change the most between the different networks (rewired) The higher the rewiring score, the more the gene's co-expression with other genes varies between conditions. Diffany is another tool that was used in order to compare networks that functions differently than DyNet [47]. Diffany was used to generate a directional network that visualizes how the correlations between genes changes between the normal and afflicted (MCI and AD) states. The steps from data acquisition to network creation are detailed in Figure 5 below.

A



B



C

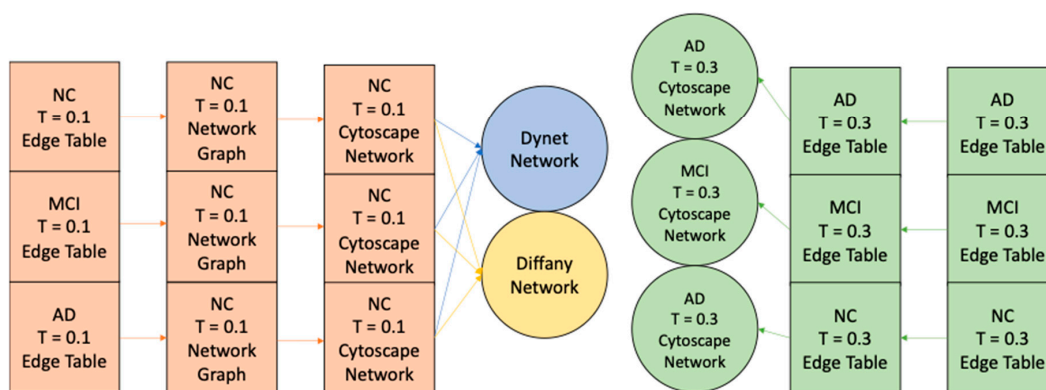


**Figure 5.** The general process for retrieving, processing and ultimately turning Alzheimer’s Disease Neuroimaging Initiative (ADNI) gene expression data into their corresponding networks. (A) General process for acquisition/processing and gene filtration. (B) General process for transforming expression data to edge tables. The process is the same for both positive and negative correlation matrices/networks, only the sign and direction of the threshold is changed. e.g.,  $>0.3$  for positive correlation,  $<-0.3$  for negative correlation. (C) General process for transforming gene expression data from edge tables to networks. The process is the same for both positive and negative correlation matrices/networks, only the sign of the threshold is changed. e.g.,  $>0.3$  for positive correlation,  $<-0.3$  for negative correlation.  $T = 0.1$  edge tables were used for the DyNet (Figure 1) and Diffany (Figure 2) networks,  $T = 0.3$  edge tables were used for the basic networks (Figures 3 and 4).

## 5. Conclusions

Conducting a network-based analysis of the gene expression levels and the co-expression patterns observed between samples in blood samples obtained from NC, MCI, and AD subjects has proven to be fairly productive. In addition to reinforcing some of the research performed on many of the genes already, this work and other network-based analysis serve to elucidate some other potential genes and pathways for further study; many of the connections are not obvious at a glance. All of the genes examined in this study exhibited aberrant expression levels in those with Alzheimer's disease and mild cognitive impairment. While some may have not been connected on the networks examined in this study, this does not necessarily mean it is insignificant nor that it exhibits no patterns of co-expression. They may be related to other genes that were excluded in this study, due to the filtration applied or limitations of the microarray analysis. Additionally, this study examined genes found in the subject's blood, which may not translate directly to expression within the subject's brain in all cases. Many of the known key players in Alzheimer's disease, such as APP, are differentially expressed between tissue types and between different regions of the brain [48]. With that being said, with further study these genes may prove to be valuable biomarkers for use in much-needed early diagnosis tests, as many of the genes show similar expression patterns and relationships in both MCI and AD individuals and blood is a relatively easily obtained sample.

**Supplementary Materials:** Supplementary materials can be found at <http://www.mdpi.com/1422-0067/21/1/332/s1>.

**Author Contributions:** Conceptualization, X.H.; methodology, D.C. and A.P.; formal analysis, D.C. and A.P.; software, D.C. and A.P.; validation, D.C. and A.P.; investigation, D.C. and A.P.; resources, X.H.; writing—original draft preparation, D.C. and A.P.; visualization, D.C. and A.P.; supervision, X.H.; project administration, X.H.; funding acquisition, X.H.; writing—review and editing, X.H. All authors have read and agreed to the published version of the manuscript.

**Funding:** This work was supported in part by a NIH grant- R01AG056614.

**Acknowledgments:** Data used in preparation of this article were obtained from the Alzheimer's Disease Neuroimaging Initiative (ADNI) database ([adni.loni.usc.edu](http://adni.loni.usc.edu)). As such, the investigators within the ADNI contributed to the design and implementation of ADNI and/or provided data but did not participate in analysis or writing of this report. A complete listing of ADNI investigators can be found at: [http://adni.loni.usc.edu/wpcontent/uploads/how\\_to\\_apply/ADNI\\_Acknowledgement\\_List.pdf](http://adni.loni.usc.edu/wpcontent/uploads/how_to_apply/ADNI_Acknowledgement_List.pdf). Data collection and sharing for this project was funded by the ADNI (National Institutes of Health Grant U01 AG024904) and DOD ADNI (Department of Defense award number W81XWH-12-2-0012). ADNI is funded by the National Institute on Aging, the National Institute of Biomedical Imaging and Bioengineering, and through generous contributions from the following: AbbVie, Alzheimer's Association; Alzheimer's Drug Discovery Foundation; Araclon Biotech; BioClinica, Inc.; Biogen; Bristol-Myers Squibb Company; CereSpir, Inc.; Cogstate; Eisai Inc.; Elan Pharmaceuticals, Inc.; Eli Lilly and Company; EuroImmun; F. Hoffmann-La Roche Ltd. and its affiliated company Genentech, Inc.; Fujirebio; GE Healthcare; IXICO Ltd.; Janssen Alzheimer Immunotherapy Research & Development, LLC.; Johnson & Johnson Pharmaceutical Research & Development LLC.; Lumosity; Lundbeck; Merck & Co., Inc.; Meso Scale Diagnostics, LLC.; NeuroRx Research; Neurotrack Technologies; Novartis Pharmaceuticals Corporation; Pfizer Inc.; Piramal Imaging; Servier; Takeda Pharmaceutical Company; and Transition Therapeutics. The Canadian Institutes of Health Research is providing funds to support ADNI clinical sites in Canada. Private sector contributions are facilitated by the Foundation for the National Institutes of Health ([www.fnih.org](http://www.fnih.org)). The grantee organization is the Northern California Institute for Research and Education, and the study is coordinated by the Alzheimer's Therapeutic Research Institute at the University of Southern California. ADNI data are disseminated by the Laboratory for Neuro Imaging at the University of Southern California.

**Conflicts of Interest:** The authors declare no conflict of interest. The funders had no role in the design of the study; in the collection, analysis, or interpretation of data; in the writing of the manuscript, or in the decision to publish the results.

## Abbreviations

AD	Alzheimer's disease
ADNI	Alzheimer's Disease Neuroimaging Initiative
CBS	Cystathionine beta synthase
FDR	False discovery rate
HP	Haptoglobin
lncRNA	Long non-coding RNA
MCI	Mild cognitive impairment
MHC	Major Histocompatibility Complex
NC	Normal condition
NM	Network medicine
PTGDS	Prostaglandin D2 synthase
XIST	X-inactive specific transcript

## References

1. Alzheimer's Association. 2016 Alzheimer's disease facts and figures. *Alzheimer's Dement.* **2016**, *12*, 459–509. [[CrossRef](#)]
2. Hebert, L.E.; Weuve, J.; Scherr, P.A.; Evans, D.A. Alzheimer disease in the United States (2010–2050) estimated using the 2010 census. *Neurology* **2013**, *80*, 1778–1783. [[CrossRef](#)]
3. Weiner, M.W.; Veitch, D.P.; Aisen, P.S.; Beckett, L.A.; Cairns, N.J.; Green, R.C.; Harvey, D.; Jack, C.R., Jr.; Jagust, W.; Morris, J.C.; et al. Recent publications from the Alzheimer's Disease Neuroimaging Initiative: Reviewing progress toward improved AD clinical trials. *Alzheimer's Dement.* **2017**, *13*, e1–e85. [[CrossRef](#)]
4. Loscalzo, J.; Barabasi, A.L.; Silverman, E.K. *Network Medicine: Complex Systems in Human Disease and Therapeutics*; Harvard University Press: Cambridge, MA, USA, 2017.
5. Barabasi, A.L.; Gulbahce, N.; Loscalzo, J. Network medicine: A network-based approach to human disease. *Nat. Rev. Genet.* **2011**, *12*, 56–68. [[CrossRef](#)] [[PubMed](#)]
6. Jarrell, J.T.; Gao, L.; Cohen, D.S.; Huang, X. Network Medicine for Alzheimer's Disease and Traditional Chinese Medicine. *Molecules* **2018**, *23*, 1143. [[CrossRef](#)] [[PubMed](#)]
7. Hu, Y.S.; Xin, J.; Hu, Y.; Zhang, L.; Wang, J. Analyzing the genes related to Alzheimer's disease via a network and pathway-based approach. *Alzheimer's Res. Ther.* **2017**, *9*, 29. [[CrossRef](#)] [[PubMed](#)]
8. Hu, W.; Lin, X.; Chen, K. Integrated analysis of differential gene expression profiles in hippocampi to identify candidate genes involved in Alzheimer's disease. *Mol. Med. Rep.* **2015**, *12*, 6679–6687. [[CrossRef](#)] [[PubMed](#)]
9. Silverman, E.K.; Loscalzo, J. Network medicine approaches to the genetics of complex diseases. *Discov. Med.* **2012**, *14*, 143–152.
10. Hosp, F.; Vossfeldt, H.; Heinig, M.; Vasiljevic, D.; Arumughan, A.; Wyler, E.; Genetic and Environmental Risk for Alzheimer's Disease GERAD1 Consortium; Landthaler, M.; Hubner, N.; Wanker, E.E.; et al. Quantitative interaction proteomics of neurodegenerative disease proteins. *Cell Rep.* **2015**, *11*, 1134–1146. [[CrossRef](#)]
11. Kitsak, M.; Sharma, A.; Menche, J.; Guney, E.; Ghiassian, S.D.; Loscalzo, J.; Barabasi, A.L. Tissue Specificity of Human Disease Module. *Sci. Rep.* **2016**, *6*, 35241. [[CrossRef](#)]
12. Siavelis, J.C.; Bourdakou, M.M.; Athanasiadis, E.I.; Spyrou, G.M.; Nikita, K.S. Bioinformatics methods in drug repurposing for Alzheimer's disease. *Brief. Bioinform.* **2016**, *17*, 322–335. [[CrossRef](#)] [[PubMed](#)]
13. Mostafavi, S.; Gaiteri, C.; Sullivan, S.E.; White, C.C.; Tasaki, S.; Xu, J.; Taga, M.; Klein, H.U.; Patrick, E.; Komashko, V.; et al. A molecular network of the aging human brain provides insights into the pathology and cognitive decline of Alzheimer's disease. *Nat. Neurosci.* **2018**, *21*, 811–819. [[CrossRef](#)] [[PubMed](#)]
14. Song, I.U.; Kim, Y.D.; Chung, S.W.; Cho, H.J. Association between serum haptoglobin and the pathogenesis of Alzheimer's disease. *Intern. Med.* **2015**, *54*, 453–457. [[CrossRef](#)] [[PubMed](#)]
15. Zhu, C.; Jiang, G.; Chen, J.; Zhou, Z.; Cheng, Q. Serum haptoglobin in Chinese patients with Alzheimer's disease and mild cognitive impairment: A case-control study. *Brain Res. Bull.* **2018**, *137*, 301–305. [[CrossRef](#)]
16. Yang, H.; Wang, H.; Wang, Y.; Addorisio, M.; Li, J.; Postiglione, M.J.; Chavan, S.S.; Al-Abed, Y.; Antoine, D.J.; Andersson, U.; et al. The haptoglobin beta subunit sequesters HMGB1 toxicity in sterile and infectious inflammation. *J. Intern. Med.* **2017**, *282*, 76–93. [[CrossRef](#)]

17. Holmes, C. Review: Systemic inflammation and Alzheimer's disease. *Neuropathol. Appl. Neurobiol.* **2013**, *39*, 51–68. [[CrossRef](#)]
18. Corrada, M.M.; Kawas, C.H.; Hallfrisch, J.; Muller, D.; Brookmeyer, R. Reduced risk of Alzheimer's disease with high folate intake: The Baltimore Longitudinal Study of Aging. *Alzheimer's Dement.* **2005**, *1*, 11–18. [[CrossRef](#)]
19. Sonkar, S.K.; Kumar, S.; Singh, N.K.; Tandon, R. Hyperhomocysteinemia induced locked-in syndrome in a young adult due to folic acid deficiency. *Nutr. Neurosci.* **2019**. [[CrossRef](#)]
20. Loera-Valencia, R.; Goikolea, J.; Parrado-Fernandez, C.; Merino-Serrais, P.; Maioli, S. Alterations in cholesterol metabolism as a risk factor for developing Alzheimer's disease: Potential novel targets for treatment. *J. Steroid Biochem. Mol. Biol.* **2019**, *190*, 104–114. [[CrossRef](#)]
21. Beyer, K.; Lao, J.I.; Carrato, C.; Rodriguez-Vila, A.; Latorre, P.; Mataro, M.; Llopis, M.A.; Mate, J.L.; Ariza, A. Cystathionine beta synthase as a risk factor for Alzheimer disease. *Curr. Alzheimer Res.* **2004**, *1*, 127–133. [[CrossRef](#)]
22. McCarty, M.; O'Keefe, J.; DiNicolantonio, J. A diet rich in taurine, cysteine, folate B12 and betaine may lessen risk for Alzheimer's disease by boosting brain synthesis of hydrogen sulfide. *Med. Hypotheses* **2019**, *132*, 109356. [[CrossRef](#)] [[PubMed](#)]
23. Shi, M.T.; Zhang, Y.; Zhou, G.Q. The critical roles of TBC proteins in human diseases. *Yi Chuan Hered.* **2018**, *40*, 12–21.
24. Tam, K.T.; Chan, P.K.; Zhang, W.; Law, P.P.; Tian, Z.; Fung Chan, G.C.; Philipsen, S.; Festenstein, R.; Tan-Un, K.C. Identification of a novel distal regulatory element of the human Neuroglobin gene by the chromosome conformation capture approach. *Nucleic Acids Res.* **2017**, *45*, 115–126. [[CrossRef](#)] [[PubMed](#)]
25. Gray, K.; Stefen, H.; Ly, T.; Keller, C.; Colpan, M.; Wayman, G.; Pate, E.; Fath, T.; Kostyukova, A. Tropomodulin's actin-binding abilities are required to modulate dendrite development. *Front. Mol. Neurosci.* **2018**, *11*, 357. [[CrossRef](#)] [[PubMed](#)]
26. Fagerberg, L.; Hallstrom, B.M.; Oksvold, P.; Kampf, C.; Djureinovic, D.; Odeberg, J.; Habuka, M.; Tahmasebpoor, S.; Danielsson, A.; Edlund, K.; et al. Analysis of the human tissue-specific expression by genome-wide integration of transcriptomics and antibody-based proteomics. *Mol. Cell Proteom.* **2014**, *13*, 397–406. [[CrossRef](#)] [[PubMed](#)]
27. Luna, R.E.; Arthanari, H.; Hiraishi, H.; Akabayov, B.; Tang, L.; Cox, C.; Markus, M.A.; Luna, L.E.; Ikeda, Y.; Watanabe, R.; et al. The interaction between eukaryotic initiation factor 1A and eIF5 retains eIF1 within scanning preinitiation complexes. *Biochemistry* **2013**, *52*, 9510–9518. [[CrossRef](#)] [[PubMed](#)]
28. Rauschendorf, M.A.; Zimmer, J.; Hanstein, R.; Dickemann, C.; Vogt, P.H. Complex transcriptional control of the AZFa gene DDX3Y in human testis. *Int. J. Androl.* **2011**, *34*, 84–96. [[CrossRef](#)]
29. Baarends, W.M.; van der Laan, R.; Grootegoed, J.A. Specific aspects of the ubiquitin system in spermatogenesis. *J. Endocrinol. Investig.* **2000**, *23*, 597–604. [[CrossRef](#)]
30. Komura, K.; Yoshikawa, Y.; Shimamura, T.; Chakraborty, G.; Gerke, T.A.; Hinohara, K.; Chadalavada, K.; Jeong, S.H.; Armenia, J.; Du, S.Y.; et al. ATR inhibition controls aggressive prostate tumors deficient in Y-linked histone demethylase KDM5D. *J. Clin. Investig.* **2018**, *128*, 2979–2995. [[CrossRef](#)]
31. Chen, X.; Tong, C.; Li, H.; Peng, W.; Li, R.; Luo, X.; Ge, H.; Ran, Y.; Li, Q.; Liu, Y.; et al. Dysregulated Expression of RPS4Y1 (Ribosomal Protein S4, Y-Linked 1) Impairs STAT3 (Signal Transducer and Activator of Transcription 3) Signaling to Suppress Trophoblast Cell Migration and Invasion in Preeclampsia. *Hypertension* **2018**, *71*, 481–490. [[CrossRef](#)]
32. Forese, M.G.; Pellegatta, M.; Canevazzi, P.; Gullotta, G.S.; Podini, P.; Rivellini, C.; Previtali, S.C.; Bacigaluppi, M.; Quattrini, A.; Taveggia, C. Prostaglandin D2 synthase modulates macrophage activity and accumulation in injured peripheral nerves. *Glia* **2020**, *68*, 95–110. [[CrossRef](#)] [[PubMed](#)]
33. Bulow, S.; Zeller, L.; Werner, M.; Toelge, M.; Holzinger, J.; Entzian, C.; Shubert, T.; Waldow, F.; Gisch, N.; Hammerschmidt, S. Bactericidal/Permeability-increasing Protein is an Enhancer of Bacterial Lipoprotein Recognition. *Front. Immunol.* **2018**, *9*, 2768. [[CrossRef](#)] [[PubMed](#)]
34. Brice, D.; Diamond, G. Antiviral Activities of Human Host Defense Peptides. *Curr. Med. Chem.* **2019**. [[CrossRef](#)] [[PubMed](#)]
35. Huntoon, K.; Wang, Y.; Eppolito, C.; Barbour, K.; Berger, F.; Shrikant, P.; HBaumann, H. The acute phase protein haptoglobin regulates host immunity. *J. Leukoc. Biol.* **2008**, *84*, 170–181. [[CrossRef](#)]

36. McGeer, P.; Akiyama, H.; Itagaki, S.; McGeer, E. Immune system response in Alzheimer's disease. *Can. J. Neurol. Sci.* **1989**, *16*, 516–527. [[CrossRef](#)]
37. Jiang, J.; Natarajan, K.; Marguilies, D. MHC molecules, T cell receptors, natural killer cell receptors, and viron immunoevasins-key elements of adaptive and innate immunity. *Adv. Exp. Med. Biol.* **2019**, *1172*, 21–62.
38. Loda, A.; Heard, E. Xist RNA in action: Past, present, and future. *PLoS Genet.* **2019**, *15*, e1008333. [[CrossRef](#)]
39. Tang, L.; Liu, L.; Li, G.; Jiang, P.; Wang, Y.; Li, J. Expression Profiles of Long Noncoding RNAs in Intranasal LPS-Mediated Alzheimer's Disease Model in Mice. *Biomed. Res. Int.* **2019**, *2019*, 9642589. [[CrossRef](#)]
40. Rondinelli, B.; Rosano, D.; Antonini, E.; Frenquelli, M.; Montanini, L.; Huang, D.; Segalla, S.; Yoshihara, K.; Amin, S.; Lazarevic, D.; et al. Histone demethylase JARID1C inactivation triggers genomic instability in sporadic renal cancer. *J. Clin. Investig.* **2015**, *125*, 4625–4637. [[CrossRef](#)]
41. LaSalle, J.M.; Powell, W.T.; Yasui, D.H. Epigenetic layers and players underlying neurodevelopment. *Trends Neurosci.* **2013**, *36*, 460–470. [[CrossRef](#)]
42. Jack, C.R., Jr.; Bernstein, M.A.; Fox, N.C.; Thompson, P.; Alexander, G.; Harvey, D.; Borowski, B.; Britson, P.J.; Whitwell, J.L.; Ward, C.; et al. The Alzheimer's Disease Neuroimaging Initiative (ADNI): MRI methods. *J. Magn. Reson. Imaging* **2008**, *27*, 685–691. [[CrossRef](#)] [[PubMed](#)]
43. Weiner, M.W.; Veitch, D.P.; Aisen, P.S.; Beckett, L.A.; Cairns, N.J.; Cedarbaum, J.; Green, R.C.; Harvey, D.; Jack, C.R.; Jagust, W.; et al. 2014 Update of the Alzheimer's Disease Neuroimaging Initiative: A review of papers published since its inception. *Alzheimer's Dement.* **2015**, *11*, e1–e120. [[CrossRef](#)] [[PubMed](#)]
44. Saykin, A.J.; Shen, L.; Yao, X.; Kim, S.; Nho, K.; Risacher, S.L.; Ramanan, V.K.; Foroud, T.M.; Faber, K.M.; Sarwar, N.; et al. Genetic studies of quantitative MCI and AD phenotypes in ADNI: Progress, opportunities, and plans. *Alzheimer's Dement.* **2015**, *11*, 792–814. [[CrossRef](#)] [[PubMed](#)]
45. Mar, J.C.; Matigian, N.A.; Mackay-Sim, A.; Mellick, G.D.; Sue, C.M.; Silburn, P.A.; McGrath, J.J.; Quackenbush, J.; Wells, C.A. Variance of gene expression identifies altered network constraints in neurological disease. *PLoS Genet.* **2011**, *7*, e1002207. [[CrossRef](#)]
46. Shannon, P.; Markiel, A.; Ozier, O.; Baliga, N.S.; Wang, J.T.; Ramage, D.; Amin, N.; Schwikowski, B.; Ideker, T. Cytoscape: A software environment for integrated models of biomolecular interaction networks. *Genome Res.* **2003**, *13*, 2498–2504. [[CrossRef](#)]
47. Van Landeghem, S.; Van Parys, T.; Dubois, M.; Inze, D.; Van de Peer, Y. Diffany: An ontology-driven framework to infer, visualise and analyse differential molecular networks. *BMC Bioinform.* **2016**, *17*, 18. [[CrossRef](#)]
48. Aguirre-Plans, J.; Pinero, J.; Menche, J.; Sanz, F.; Furlong, L.I.; Schmidt, H.; Oliva, B.; Guney, E. Proximal Pathway Enrichment Analysis for Targeting Comorbid Diseases via Network Endopharmacology. *Pharmaceuticals* **2018**, *11*, 61. [[CrossRef](#)]

